Int J Adv Manuf Technol
DOI 10.1007/s00170-016-9763-1

ORIGINAL ARTICLE

The Monge theorem and its application in engineering practice

Zsuzsanna Balajti[1,2] · **Illés Dudás**[1,3]

Received: 22 March 2016 / Accepted: 11 November 2016

Abstract Engineering innovation activities cannot be performed without mathematical devices. The present paper describes the theoretical analysis of the reconstruction of the Monge theorem. The significance of the analysis is that we consider those Monge projections the same, which can be translated to one another by parallel shifting. Accordingly, in a fixed Descartes coordinate system in the space, every Monge projection is determined by its two projection lines that go through the origin point, which is described by three free parameters. The three free parameters determining the Monge projections make up the points of the Monge cuboid. We are looking for Monge projections to a fixed third-grade spatial curve, in which the reconstruction of the curve can be carried out only with two pictures without any further information. The inner points of the Monge cuboid—defined by the bijective Monge projections—are bordered by a surface. This surface is described in this article during our research work first. We have proved the engineering application of this theorem by calculating the correct camera position for the wearing examination of the hob's cutting edge.

Keywords Monge · Worm gear · Hob · Projection

✉ Illés Dudás
illes.dudas@uni-miskolc.hu

Zsuzsanna Balajti
balajtizsuzsanna@gmail.com

[1] Faculty of Mechanical Engineering and Informatics, University of Miskolc, Egyetemváros, Miskolc 3515, Hungary

[2] Department of Descriptive Geometry, University of Miskolc, Egyetemváros, Miskolc 3515, Hungary

[3] Department of Production Technology, Institute of Manufacturing Science, Egyetemváros, Miskolc 3515, Hungary

Abbreviation

P	Point
e	Line
$\underline{S}$	Plane
~~o~~	Fitting
$\underline{o}$	Non-fitting
$\underline{K}_1$, $\underline{K}_2$	Image planes
v_1, v_2	Projection lines
$\underline{P}$	Profile plane
$\underline{N}$	Normal plane
O(xyz)	Coordinate system
$K_1(x_1, y_1, z_1)$	Stationary coordinate system connected to helicoid surface
$K_{F1}(x_{F1}y_{F1}z_{F1})$	Rotating coordinate system affixed helicoid surface
[…]	Plane with its identifying spatial elements in the square brackets
[xy]	Coordinate plane fitting to axes x and y
[yz]	Coordinate plane fitting to axes y and z
[zx]	Coordinate plane fitting to axes z and x
α (rad)	First direction angle
β (rad)	Second direction angle
γ (rad)	Third direction angle
ω	Angle between the axis and a generating line of the cone created Tangents of helicoid
δ	Angle between the axis of the helicoid and the projection direction
g	Curve
u	Parameter
$\underline{r}$(u)	Function in case its scalar values are made from set of vectors
$\underline{e}$	Tangent vector
$\underline{n}$	Normal vector
p	Helicoid parameter
h (mm)	Internal parameter of helicoid surface

Published online: 28 November 2016

q (rad)	Internal parameter of helicoid surface
f (rad)	Angular displacement of helicoid surface
p_h	Screw parameter of the face surface
d_{01} (mm)	Mid-cylinder diameter
γ_{0h} (rad)	Mid-cylinder lead angle
z_{ax} (mm)	Axial translation of coordinate system to the machining position in case helicoid surface
ρ_{ax} (mm)	Arc radius in axial section
K (mm)	Distance between the centre of profile circle and axis of worm
H	Face surface of the hob
R	Backward grinded side surface
V	Cutting edge of the hob

1 Introduction

Several theories for the modelling of the spatial figures have been developed, which we hold in great esteem. [1–3]. The theory we have developed ensures the reconstruction from two photos by the application of complex geometric devices in order to examine changes in size. The representation of a point in Monge projection is unambiguous provided that the well-known conventions are fulfilled [4].

Due to the practice of descriptive geometry, anomalies occur during the representation of lines, of which we have to be aware. For example the representation of a circle of general position and a profile line is not bijective. For such and similar cases, descriptive geometry found special solutions to ensure bijectivity.

The need for an examination of bijectivity at present has been brought about by the demand for reconstruction based on digitized Monge projections [5, 6, 13].

Two perpendicular projections are not different, if they can be translated to each other in practice [4, 7, 8].

As long as we consider that Monge projections, which can be translated into each other, are identical, the number of Monge projections to a given curve can be described by using three free real parameters that we have defined.

Each Monge projection corresponds to a point of a rectangular prism. We call such a rectangular prism a Monge cuboid. Each point of a Monge cuboid defines a triplet of real numbers, which is in fact a triplet of angles providing us with a Monge projection with respect to a given curve [5].

The points of the Monge cuboid can be divided into two subsets. One which corresponds to bijective mappings and another which corresponds to non-bijective mappings of a given curve. The bijective subset and non-bijective subset of the inner points of the Monge cuboid are separated by a border surface.

The images done by CCD cameras from the direction of projecting lines of bijective Monge mappings are suitable for the examination of the wearing of the tool edge during the production process of worm gear drive elements. High-precision manufacturing is necessary to realize the required good efficiency, low noise level and so forth [9]. The wearing examination of the grinding wheel profile with a CCD camera was carried out in the production process in our previous research [10, 15]. In the production process, the spatial reconstruction of the cutting edge of the tool can be done by appropriately positioned CCD cameras. The cutting edge curve of the hob must be reconstructed from its two pictures taken by the CCD cameras in the finishing production of the worm gear tooth surface for the wearing examination. The conditions of the unambiguous reconstruction have been determined in case of Hermite line in our previous research [5, 7]. The positions of the CCD cameras have been determined by the application of correctly selected interpolation curve fitting to the cutting edge in order to ensure reconstruction. The points of the bijective part of the Monge cuboid give us the right positions of the CCD cameras concerning the cutting edge of the hob in the manufacturing process.

2 Definition of the Monge cuboid

2.1 Definitions of direction angles of the line

The definitions were prepared using a fixed Descartes coordinate system O(x, y, z).

Definition 1 The first direction angle α ($0 \le \alpha \le \pi$) of the line e fitting O origin point is that angle, with which the axis x^+ can be turned to the first projection e′ of the line on the plane [xy] to the direct y^+ (Fig. 1). Let $\alpha = 0$, if the line e is identical to axis. First direction angle of a line missing O is identical with first directional angle of its parallel line fitting O.

Definition 2 The second direction angle β ($0 \le \beta \le \pi$) of the line e fitting O origin point is the angle with which the axis y^+ can be turned to the second projection e″ of the line on the plane [yz] to the direct z^+ (Fig. 1). Let $\beta = 0$, if the line e is identical to axis x. Second direction angle of a line missing O is identical with second directional angle of its parallel line fitting O.

Definition 3 The third direction angle γ ($0 \le \gamma \le \pi$) of the line e fitting O origin point is the angle with which the axis z^+ can be turned to the third projection e‴ of the line on the plane [zx] to the direct x^+ (Fig. 1). Let $\gamma = 0$, if the line e is identical to axis y. Third direction angle of a line missing O is identical with the third directional angle of its parallel line fitting O.

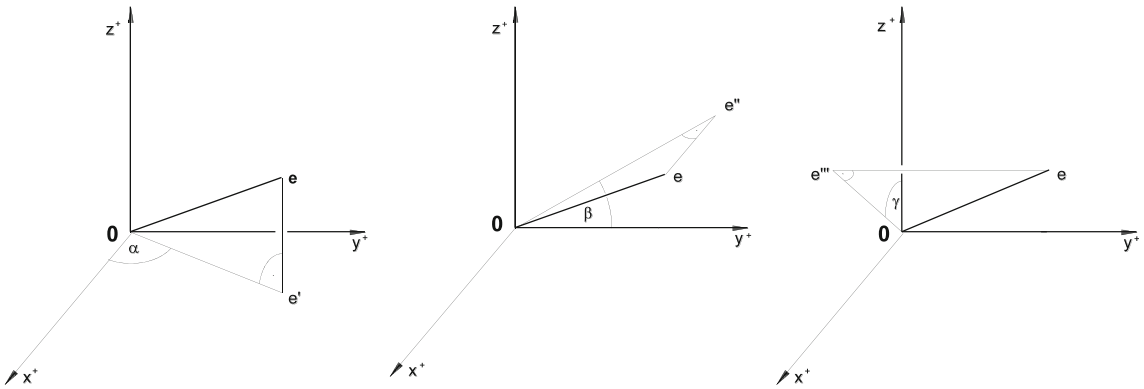

Fig. 1 The first direction angle α, the second direction angle β and the third direction angle γ of the line e

2.2 The connection between the Monge projections and the three free parameters

Definition 4 The image planes $\{\underline{K}_1, \underline{K}_2\}$ and its projection lines v_1, v_2 together have been named as a Monge projection.

The Monge projections, which can be translated to each other by parallel shifting, give us the same result considering reconstruction. Therefore, the Monge projections determined by parallel image planes and projecting lines create one class with a Monge projection passing through an origin point O of a fixed coordinate system, because they are identical from the viewpoint of our examinations.

Without Monge projections, projecting lines v_1 and v_2 satisfy conditions v_1 ~~o~~ $[z, x]$ and v_2 o $[z, x]$ together, which give us three free parameters (α, β, γ) in a fixed Descartes coordinate system O[x, y, z] in the following way:

The α is the first direction angle, the β is the second direction angle of the first projection line v_1 and the angle γ is the third direction angle of the second projection line v_2 of the Monge projection (Fig. 2). But the expounded triplet of angles (α, β, γ) determines the projection lines of the Monge projection and the Monge projection itself. The v_1 is determined by intersection of the first projection plane fitting on the v_1' and the second projection plane fitting on the v_1'' (Fig. 2). The v_2 is determined by the intersection of the normal plane $\underline{N}$ of the first projection line v_1 and the third projection plane fitting on the v_2''' (Fig. 2).

2.3 The definition of the Monge cuboid

Definition 5 The subset of values α, β, γ in interval $[0,\pi]$, to which unambiguously can be linked an Monge projection, described in an another Descartes coordinate system O[α, β, γ], is called Monge cuboid.

The inner points of the Monge cuboid (Fig. 3) satisfy the following condition

$$0 < \alpha < \pi, 0 < \beta < \pi/2, \pi/2 < \beta < \pi, 0 < \gamma < \pi. \quad (1)$$

The border points on the Monge cuboid (Fig. 3) satisfy the following conditions

$$\begin{aligned}
&\text{-}0 < \alpha < \pi, \beta = \pi, 0 < \gamma <= \pi,\\
&\text{-}0 < \alpha < \pi, 0 < \beta < \pi/2, \pi/2 < \beta <= \pi, \gamma = \pi,\\
&\text{-}\alpha = \pi, \beta = \pi/2, 0 < \gamma < \pi/2, \pi/2 < \gamma < \pi,\\
&\text{-}\ \alpha = 0\ ,\ \beta = \pi\ /\ 2\ ,\ \gamma = \pi\ /\ 2\\
&\text{-}\ \alpha = \pi\ ,\ \beta = 0\ ,\ \gamma = \pi\ .
\end{aligned} \quad (2)$$

In summary, all image planes $\{\underline{K}_1, \underline{K}_2\}$ and projection lines v_1 and v_2, which can be translated into each other with parallel

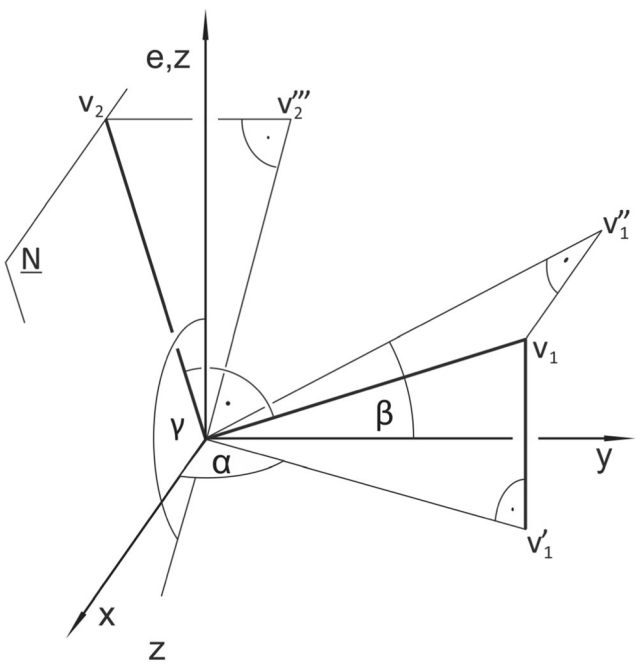

Fig. 2 The relation between the triplet of angles (α, β, γ) and the projection lines v_1 and v_2 of Monge projections in the fixed Descartes coordinate system O[x, y, z]

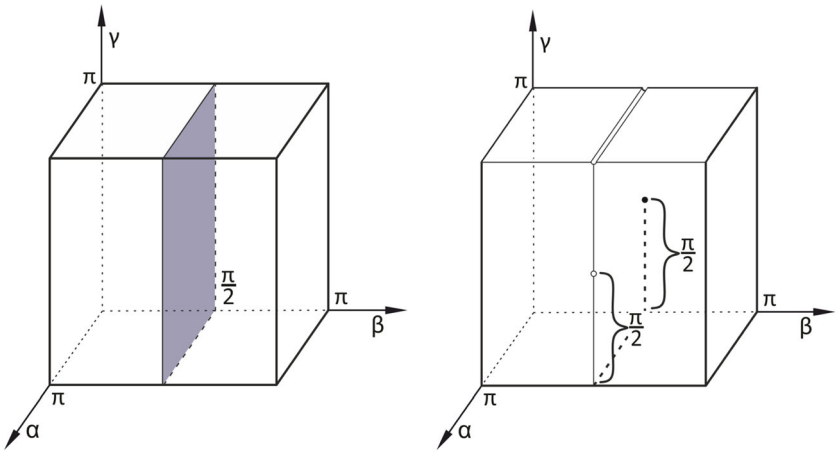

Fig. 3 The inner points and the border points of the Monge cuboid

dislocation, are members of a class of the Monge mappings considering our approach. We have named this class Monge projection. In this approach, Monge projections can be described by using three free real parameters that we have defined. These triplets of numbers create the Monge cuboid.

One Monge projection corresponds to a point of Monge cuboid in a defined way. In the opposite direction, each point of a Monge cuboid defines a triplet of real numbers which is in fact a triplet of angles providing us with a Monge projection.

The ordering between the Monge projections and the point of the Monge cuboid is a mathematical mapping.

This method does not discuss all Monge projections but discusses all two perpendicular projections that are relevant in engineering work, and this is enough for our examination, because the examination of the bijectivity with respect to a given curve gives us the same result if the first and second images are changed [5, 7, 8].

3 About the bijectivity of curve mappings

Theorem 1 If the curve has not got tangent line in profile position, then any part of it can be reconstructed from its two pictures (Fig. 4).

Proof If the g curve has not got tangent in profile position, it means that tangent in any point P_0 with u_0 parameter on its image curves is not position in projection line, namely the projection line cuts the curve in its any point P_0. Consequently, such a point as P_0 does not exist with parameter u_0 of the curve g, in which neighbouring point P_{-1} with parameter u_{-1} and point P_1 with parameter u_1 are located in the same side of the projection line of the P_0, where $u_{-1} < u_0 < u_1$. This means that a piece of curve, which has two points on a projection line, does not exist. Namely, all projection lines have only one point of the curve, so any point of the curve can be reconstructed from its two pictures, which means that the description of the curve is bijective.

Theorem 2 If image curves g' and g'' of the curve g that corresponded on the Descartes coordinate planes cannot be written as function $x = f_1(y)$ and $z = f_2(y)$, namely $y \rightarrow f_1(y)$ and $y \rightarrow f_2(y)$ are not functions, then a piece of the curve g exists, which cannot be reconstructed from the two pictures unambiguously (Fig. 5).

Proof Because the curve g and its image curves g' and g'' cannot be written as functions—but of course they are curves—in the suitable Descartes coordinate planes, one coordinate y is connected more $f_1(y) \equiv P'$ fitting on the plane $[xy] \equiv \underline{K}_1$ and more $f_2(y) \equiv P''$ fitting on the plane $[y, z] \equiv \underline{K}_2$. These P' and P'' lying on the perpendicular line to the axis $y \equiv x_{12}$ can be ordered to each other optionally to create well ordered pairs of points, to which P points in the space are ordered. Consequently, the curve g has such a point and neighbour of the point, which cannot be reconstructed from only two pictures correctly. In this case, tangent of the curve g directed toward of a profile line exists.

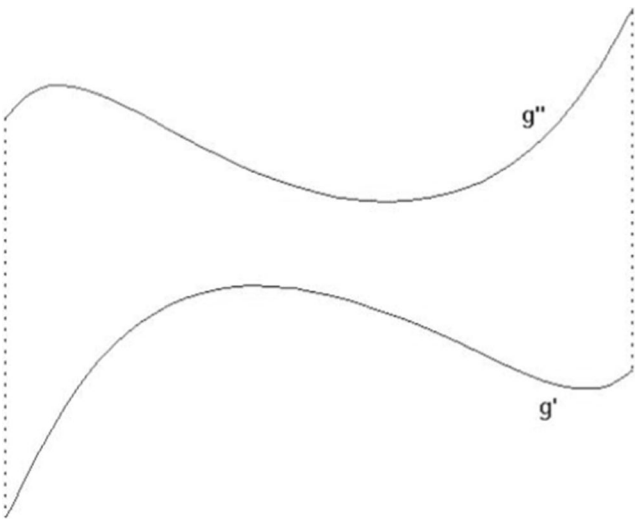

Fig. 4 Bijective mapping of g curve

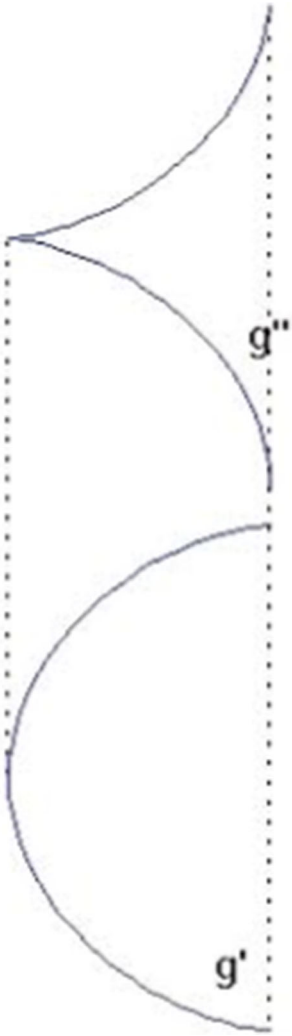

Fig. 5 Non-bijective mapping of g curve

4 The bijectivity of the cubic curve

Theorem 3 The bijective and the non-bijective subsets of inner points of the Monge cuboid with respect to a given cubic Bezier curve are bordered by points of second degree surfaces.

Proof The Bezier curve is interpolated to the given points $\underline{p}_0$, $\underline{p}_1$, $\underline{p}_2$, $\underline{p}_3$ and let the parameters u_0, u_1, u_2, u_3, where $u_i \neq u_j$, if the $i \neq j$, and $u_0 = 0$, $u_3 = 1$. We have to find control points $\underline{b}_0$, $\underline{b}_1$, $\underline{b}_2$, $\underline{b}_3$, which determine the interpolation Bezier curve fitting to $\underline{p}_0$, $\underline{p}_1$, $\underline{p}_2$, $\underline{p}_3$.

We are looking for control points $\underline{b}_0$, $\underline{b}_1$, $\underline{b}_2$, $\underline{b}_3$, which determine the Bezier curve fitting to points $\underline{p}_0$, $\underline{p}_1$, $\underline{p}_2$, $\underline{p}_3$, so

$$b(u_i) = p_i \quad (i = 0, \ldots, 3). \tag{3}$$

The equation of the Bezier curve is determined in the following formula

$$\underline{b}(u) = \sum_{j=0}^{n} B_j^n(u)\, \underline{b}_j, \tag{4}$$

where $B_j^n(u) = (n\ j)u^j(1-u)^{n-j}$ are Bernstein polynomial.

As it was mentioned earlier, the Bezier curve fitting to the given points can be described in the following equation

$$\underline{b}(u_i) = \sum_{j=0}^{n} B_j^n(u_i)\, \underline{b}_j, \quad (i = 0, ..., 3). \tag{5}$$

Using the $\underline{b}(u_i) = \underline{p}_i$ $(i = 0,\ldots,3)$ equations, we can get the following linear inhomogeneous equation system

$$\begin{bmatrix} \underline{p}_0 \\ \underline{p}_1 \\ \underline{p}_2 \\ \underline{p}_3 \end{bmatrix} = \begin{bmatrix} B_0^3(u_0) & B_1^3(u_0) & B_2^3(u_0) & B_3^3(u_0) \\ B_0^3(u_1) & B_1^3(u_1) & B_2^3(u_1) & B_3^3(u_1) \\ B_0^3(u_2) & B_1^3(u_2) & B_2^3(u_2) & B_3^3(u_2) \\ B_0^3(u_3) & B_1^3(u_3) & B_2^3(u_3) & B_3^3(u_3) \end{bmatrix} \begin{bmatrix} \underline{b}_0 \\ \underline{b}_1 \\ \underline{b}_2 \\ \underline{b}_3 \end{bmatrix}. \tag{6}$$

The $u_i \neq u_j$ condition provides us with the result of the unambiguous solution to$\underline{b}_i$. So the $\underline{b}_i$ control points of the Bezier curve fitting to points $\underline{p}_0$, $\underline{p}_1$, $\underline{p}_2$, $\underline{p}_3$ can be gotten by (6).

According to the previous things, if the tangent of a curve directed toward projection line does not exist, then any part of the curve clearly can be reconstructed from its two pictures, namely its mapping is bijective.

The connection between the Bezier curve and the Hermite arc (Fig. 6) can be written in the following formula

$$\begin{aligned} p_0 &= b_0 \\ t_0 &= 3 \cdot b_1 - 3 \cdot b_0 \\ p_3 &= \quad b_3 \\ t_3 &= 3 \cdot b_3 - 3 \cdot b_2 \end{aligned} \tag{7}$$

when the Hermite arc is given by points $\underline{p}_0$, $\underline{p}_3$ and tangents $\underline{t}_0$, $\underline{t}_3$, where u∈[0,1].

The Hermite arc can be written in parametric form, as

$$r(u) = a_3 \cdot u^3 + a_2 \cdot u^2 + a_1 \cdot u + a_0, \tag{8}$$

where

$$\begin{aligned} a_0 &= p_0, \\ a_1 &= p_3, \\ a_2 &= -3 \cdot p_0 + 3 \cdot p_3 - 2 \cdot t_0 - t_3, \\ a_3 &= 2 \cdot p_0 - 2 \cdot p_3 + t_0 + t_3. \end{aligned} \tag{9}$$

Tangent vectors can be described in the following form

$$r_e(u) = e_1 \cdot u^2 + e_2 \cdot u + e_3 \tag{10}$$

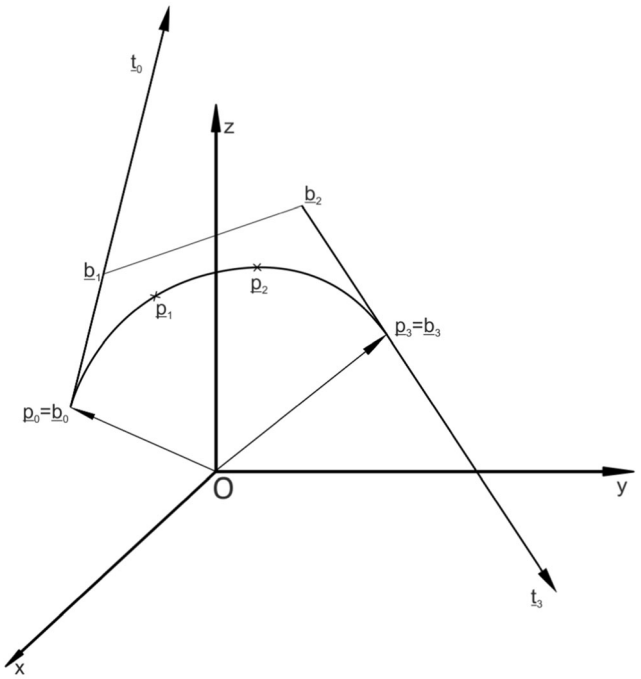

Fig. 6 The interpolation Bezier curve connecting to the Hermite arc

where

$$\begin{aligned} e_1 &= 6 \cdot p_0 - 6 \cdot p_3 + 3 \cdot t_0 + 3 \cdot t_3, \\ e_2 &= -6 \cdot p_0 + 6 \cdot p_3 - 4 \cdot t_0 - 2 \cdot t_3, \\ e_3 &= t_0. \end{aligned} \tag{11}$$

These tangent vectors pass through the origin point O. Every plane, which does not contain one of these tangent vectors, is a profile plane of a Monge projection, in which the description of the curve is bijective.

Normal vectors $\underline{n}\,(n_x, n_y, n_z)$ of planes fitting to the tangents are perpendicular to the tangents; therefore, they satisfy the following equation:

$$n \cdot r_e(u) = 0, \tag{12}$$

which can be written in the following form

$$n_x \cdot r_{ex}(u) + n_y \cdot r_{ey}(u) + n_z \cdot r_{ez}(u) = 0, \tag{13}$$

or

$$\begin{aligned} &\left(n_x \cdot e_{1x} + n_y \cdot e_{1y} + n_z \cdot e_{1z}\right) \cdot u^2 \\ &+ \left(n_x \cdot e_{2x} + n_y \cdot e_{2y} + n_z \cdot e_{2z}\right) \cdot u \\ &+ \left(n_x \cdot e_{3x} + n_y \cdot e_{3y} + n_z \cdot e_{3z}\right) \\ &= 0. \end{aligned} \tag{14}$$

We are looking for vectors $\underline{n}\,(n_x, n_y, n_z)$, to which this equation of the second degree considering parameter u in case the given e_{ij} does not have solution. Profile planes with such normal vector do not contain any tangent vectors of the given curve, namely in the Monge projection; depending on these profile planes, the description of the curve is bijective. This is only fulfilled if the discriminate of the equation of the second degree considering u is negative.

The bijective Monge projections with respect to the given curve determine a subset of the Monge cuboid. The non-bijective Monge projection with respect to the given curve determines another subset of the Monge cuboid.

The border between these subsets is given by one solution of the discriminate of the equation of the second degree considering u:

$$\begin{aligned} &\left(n_x \cdot e_{2x} + n_y \cdot e_{2y} + n_z \cdot e_{2z}\right)^2 \\ &-4 \cdot \left(n_x \cdot e_{1x} + n_y \cdot e_{1y} + n_z \cdot e_{1z}\right) \cdot \left(n_x \cdot e_{3x} + n_y \cdot e_{3y} + n_z \cdot e_{3z}\right) \\ &= 0 \end{aligned} \tag{15}$$

It can be written in the simplified form

$$\begin{aligned} &c_1 \cdot n_x^2 + c_2 \cdot n_y^2 + c_3 \cdot n_z^2 + c_{12} \cdot n_x \cdot n_y + c_{13} \cdot n_x \cdot n_z \\ &+ c_{23} \cdot n_y \cdot n_z \\ &= 0 \end{aligned} \tag{16}$$

where

$$\begin{aligned} c_1 &= e_{2x}^2 - 4 \cdot e_{1x} \cdot e_{3x}, \\ c_2 &= e_{2y}^2 - 4 \cdot e_{1y} \cdot e_{3y}, \\ c_3 &= e_{2z}^2 - 4 \cdot e_{1z} \cdot e_{3z}, \\ c_{12} &= 2 \cdot e_{2x} \cdot e_{2y} - 4 \cdot e_{1x} \cdot e_{3y} - 4 \cdot e_{1y} \cdot e_{3x}, \\ c_{13} &= 2 \cdot e_{2x} \cdot e_{2z} - 4 \cdot e_{1x} \cdot e_{3z} - 4 \cdot e_{1x} \cdot e_{3z}, \\ c_{23} &= 2 \cdot e_{2y} \cdot e_{2z} - 4 \cdot e_{1y} \cdot e_{3z} - 4 \cdot e_{1z} \cdot e_{3y}. \end{aligned} \tag{17}$$

The border between the bijective and non-bijective parts of the inner points of the Monge cuboid is created by a second degree surface based on the (16) form.

The direction vectors $\underline{v}_1$, $\underline{v}_2$ of the projection lines of the Monge projection are perpendicular to each other; therefore, they satisfy the following equation:

$$(v_1 \cdot v_2) = 0 \tag{18}$$

which can be written in the following form with coordinates:

$$v_{1x} \cdot v_{2x} + v_{1y} \cdot v_{2y} + v_{1z} \cdot v_{2z} = 0. \tag{19}$$

It can be arranged into the next equation:

$$v_{2y} = -\left(v_{1x} \cdot v_{2x} + v_{1z} \cdot v_{2z}\right) / v_{1y} \tag{20}$$

The following equations can be read from Fig. 2 in case α, β, $\gamma \neq 0$, and π:

$$\begin{aligned} \mathrm{tg}\alpha &= v_{1y}/v_{1x} \\ \mathrm{tg}\beta &= v_{1z}/v_{1y} \\ \mathrm{tg}\gamma &= v_{2x}/v_{2z}, \end{aligned}$$

and in the case α, β, $\gamma \neq \pi/2$:

$$\begin{aligned} \mathrm{ctg}\alpha &= v_{1x}/v_{1y} \\ \mathrm{ctg}\beta &= v_{1y}/v_{1z} \\ \mathrm{ctg}\gamma &= v_{2z}/v_{2x}. \end{aligned} \tag{21}$$

The normal vector $\underline{n}$ is perpendicular to the direction vectors of the projection lines, so

$$n = v_1 x v_2, \tag{22}$$

The coordinates of the normal vector can be written in the following form:

$$\begin{aligned} n_x &= v_{1y} \cdot v_{2z} - v_{2y} \cdot v_{1z} = \\ &(\mathrm{ctg}\beta + \mathrm{ctg}\alpha \cdot \mathrm{tg}\gamma + \mathrm{tg}\beta) \cdot v_{1z} \cdot v_{2z} = \\ &(\mathrm{ctg}\beta + \mathrm{ctg}\alpha \cdot \mathrm{tg}\gamma + \mathrm{tg}\beta) \cdot \mathrm{tg}\alpha \cdot \mathrm{tg}\beta \cdot \mathrm{ctg}\gamma \cdot v_{1x} \cdot v_{2x} \end{aligned} \tag{23}$$

$$\begin{aligned} n_y &= v_{1z} \cdot v_{2x} - v_{2z} \cdot v_{1x} = \\ &(\mathrm{tg}\gamma - \mathrm{ctg}\beta \cdot \mathrm{ctg}\alpha) \cdot v_{1z} \cdot v_{2z} = \\ &(\mathrm{tg}\gamma - \mathrm{ctg}\beta \cdot \mathrm{ctg}\alpha) \cdot \mathrm{tg}\alpha \cdot \mathrm{tg}\beta \cdot \mathrm{ctg}\gamma \cdot v_{1x} \cdot v_{2x}, \end{aligned} \tag{24}$$

$$n_z = v_{1x} v_{2y} - v_{2x} v_{1y} = (-\mathrm{ctg}\alpha - \mathrm{tg}\beta \cdot \mathrm{ctg}\gamma - \mathrm{tg}\alpha) \cdot v_{1x} \cdot v_{2x}. \tag{25}$$

Let us suppose that v_1 and v_2 are generally situated, so α, β, $\gamma \neq 0$, $\pi/2$, π in the following.

Because $\underline{n} \neq \underline{0}$ and the length of the $\underline{n}$ is optional except for 0, two cases are possible in our examination: n_z is a constant or n_z is 0.

1. Let $n_z = 1$, so

$$n_x / n_z = n_x = (\mathrm{tg}\alpha \cdot \mathrm{ctg}\gamma + \mathrm{tg}\beta + \mathrm{tg}\alpha \cdot \mathrm{tg}^2\beta \cdot \mathrm{ctg}\gamma)/(-\mathrm{ctg}\alpha - \mathrm{tg}\beta \cdot \mathrm{ctg}\gamma - \mathrm{tg}\alpha), \tag{26}$$

from Eqs. (20), (21), (23) and

$$n_y / n_z = n_y = (\mathrm{tg}\alpha \cdot \mathrm{tg}\beta - \mathrm{ctg}\gamma)/(-\mathrm{ctg}\alpha - \mathrm{tg}\beta \cdot \mathrm{ctg}\gamma - \mathrm{tg}\alpha), \tag{27}$$

from Eqs. (20), (21), and (24).

The border surface between the bijective and the non-bijective subsets of inner points of the Monge cuboid can be written from (16) in the following form:

$$\begin{aligned} &c_1 \cdot (\mathrm{tg}\alpha \cdot \mathrm{ctg}\gamma + \mathrm{tg}\beta + \mathrm{tg}\alpha \cdot \mathrm{tg}^2\beta \cdot \mathrm{ctg}\gamma)^2/(-\mathrm{ctg}\alpha - \mathrm{tg}\beta \cdot \mathrm{ctg}\gamma - \mathrm{tg}\alpha)^2 + \\ &c_2 \cdot (\mathrm{tg}\alpha \cdot \mathrm{tg}\beta - \mathrm{ctg}\gamma)^2/(-\mathrm{ctg}\alpha - \mathrm{tg}\beta \cdot \mathrm{ctg}\gamma - \mathrm{tg}\alpha)^2 + c_3 + \\ &c_{12} \cdot (\mathrm{tg}\alpha \cdot \mathrm{ctg}\gamma + \mathrm{tg}\beta + \mathrm{tg}\alpha \cdot \mathrm{tg}^2\beta \cdot \mathrm{ctg}\gamma) \cdot (\mathrm{tg}\alpha \cdot \mathrm{tg}\beta - \mathrm{ctg}\gamma)/(-\mathrm{ctg}\alpha - \mathrm{tg}\beta \cdot \mathrm{ctg}\gamma - \mathrm{tg}\alpha)^2 + \\ &c_{13} \cdot (\mathrm{tg}\alpha \cdot \mathrm{ctg}\gamma + \mathrm{tg}\beta + \mathrm{tg}\alpha \cdot \mathrm{tg}^2\beta \cdot \mathrm{ctg}\gamma)/(-\mathrm{ctg}\alpha - \mathrm{tg}\beta \cdot \mathrm{ctg}\gamma - \mathrm{tg}\alpha) + \\ &c_{23} \cdot (\mathrm{tg}\alpha \cdot \mathrm{tg}\beta - \mathrm{ctg}\gamma)/(-\mathrm{ctg}\alpha - \mathrm{tg}\beta \cdot \mathrm{ctg}\gamma - \mathrm{tg}\alpha) = 0. \end{aligned} \tag{28}$$

The result is a piece of a second degree surface.

2. If $n_z = 0$, let us suppose that $n_y = 1$:

Using (20), (21), (23) and (25)

$$n_x / n_y = n_x = (\mathrm{tg}\alpha \cdot \mathrm{ctg}\gamma + \mathrm{tg}\beta + \mathrm{tg}\alpha \cdot \mathrm{tg}^2\beta \cdot \mathrm{ctg}\gamma)/(\mathrm{tg}\beta \cdot \mathrm{tg}\alpha - \mathrm{ctg}\gamma). \tag{29}$$

The final result can be received with the replacement of taking (16) to (29)

$$\begin{aligned} &c_1 \cdot (\mathrm{tg}\alpha \cdot \mathrm{ctg}\gamma + \mathrm{tg}\beta + \mathrm{tg}\alpha \cdot \mathrm{tg}^2\beta \cdot \mathrm{ctg}\gamma)^2/(\mathrm{tg}\beta \cdot \mathrm{tg}\alpha - \mathrm{ctg}\gamma)^2 + c_2 + \\ &c_{12} \cdot (\mathrm{tg}\alpha \cdot \mathrm{ctg}\gamma + \mathrm{tg}\beta + \mathrm{tg}\alpha \cdot \mathrm{tg}^2\beta \cdot \mathrm{ctg}\gamma)/(\mathrm{tg}\beta \cdot \mathrm{tg}\alpha - \mathrm{ctg}\gamma) = 0. \end{aligned} \tag{30}$$

The result is a piece of a second degree surface.

5 The application in mechanical engineering practice

One of the most important research fields of the group of researchers at the Department of Production Engineering at the University of Miskolc is the development of the production geometry of worm gear drive pairs with arched profile [2, 4, 9, 11, 14]. One of the outstanding theme of the worm research is the cylindrical helicoid surface with arc profile in axial section generated by a circle with radius ρ_{ax} (Fig. 7).

The right-hand side surface of the worm in the rotating coordinate system $K_{F1}(x_{F1}, y_{F1}, z_{F1})$ can be written in the following form:

$$\left.\begin{aligned} x_{1F} &= -\eta \cdot \sin\vartheta \cdot; \\ y_{1F} &= \eta \cdot \cos\vartheta \cdot; \\ z_{1F} &= p \cdot \vartheta - \sqrt{\rho_{ax}^2 - (K - \eta)^2} \\ t_{1F} &= t_{sz} = 1. \end{aligned}\right\} \tag{31}$$

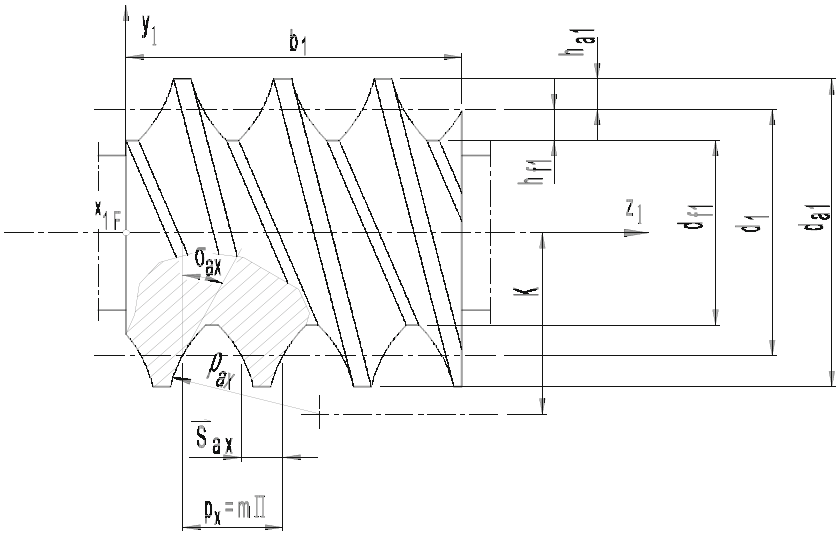

Fig. 7 The helicoid worm with arc profile in axial section [9]

The right-hand side surface of the worm in the stationary coordinate system $K_1(x_1, y_1, z_1)$ can be written in the following form:

$$\left.\begin{aligned} x_1 &= -\eta\cdot\sin\vartheta\cdot\cos\phi_1 - \eta\cdot\cos\vartheta\cdot\sin\phi_1 = -\eta\cdot\sin(\vartheta+\phi_1) \\ y_1 &= \eta\cdot\cos\vartheta\cdot\cos\phi_1 - \eta\cdot\sin\vartheta\cdot\sin\phi_1 = \eta\cdot\cos(\vartheta+\phi_1) \\ z_1 &= p\cdot(\vartheta+\phi_1) - \sqrt{\rho_{ax}^2 - (K-\eta)^2} \end{aligned}\right\} \quad (32)$$

where f_1 is the moving parameter of the worm.

Only such tool can be used to finish the tooth surface of the crown gear, which has the same covering surface as the worm mating with the gear, as it can be seen in Fig. 8 (direct movement mapping).

This tool is expedient to be the hob in case of serial production of cylindrical worm gear drives. As hobs are tools with complicated geometry and they are expensive, it is advisable to make their repeated re-sharpening possible.

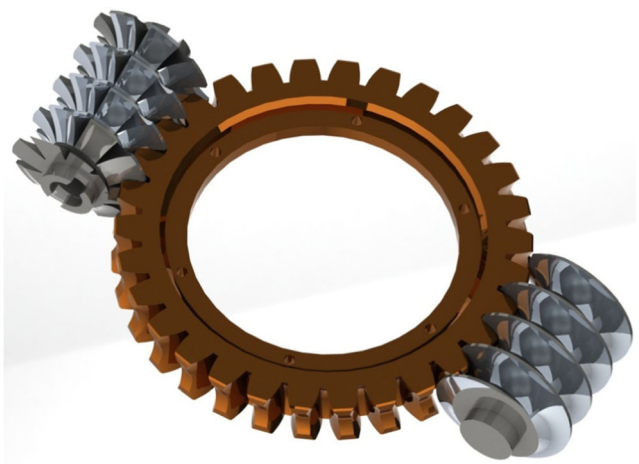

Fig. 8 The worm gear driving and the hob [11]

The cutting edge V of the hob can be obtained as an intersection of the backward grinded side surfaces R_B, R_J and the face surface H. The technology of the processing should be achieved such a way that the received edge must be on the tooth surface of the replacing worm (Fig. 9), which is geometrically the same as the tooth surface of the real worm.

The equation of the face surface H can be written in the next form

$$\left.\begin{aligned} x_h &= -\eta\cdot\sin(\vartheta+\phi_{oh}); \\ y_h &= +\eta\cdot\cos(\vartheta+\phi_{oh}); \\ z_h &= -p_h\cdot\sin(\vartheta+\phi_{oh}); \end{aligned}\right\} \quad (33)$$

where

$$p_h = \frac{d_{01}\cdot\pi\cdot\mathrm{tg}\gamma_{0h}}{2\cdot\pi} \quad (34)$$

so

$$-p_h\cdot(\vartheta+\varphi_{oh}) = p\cdot(\vartheta+\varphi_0) - \sqrt{\rho_{ax}^2-(K-\eta)^2} + z_{ax}, \quad (35)$$

from which

$$\varphi_{oh} = \frac{1}{p_h}\cdot\sqrt{\rho_{ax}^2-(K-\eta)^2} - \frac{p}{p_h}\cdot(\vartheta+\varphi_0) - \vartheta - \frac{z_{ax}}{p_h}. \quad (36)$$

The cutting edge V should remain on the replacing worm surface after re-sharpening.

The equation of the cutting edge in the examined case is the following:

$$\left.\begin{aligned} x_v &= -\eta\cdot\sin\frac{\sqrt{\rho_{ax}^2-(K-\eta)^2} - z_{ax}}{p+p_h} \\ y_v &= \eta\cdot\cos\frac{\sqrt{\rho_{ax}^2-(K-\eta)^2} - z_{ax}}{p+p_h} \\ z_v &= -p_h\cdot\frac{\sqrt{\rho_{ax}^2-(K-\eta)^2} - z_{ax}}{p+p_h} \end{aligned}\right\} \quad (37)$$

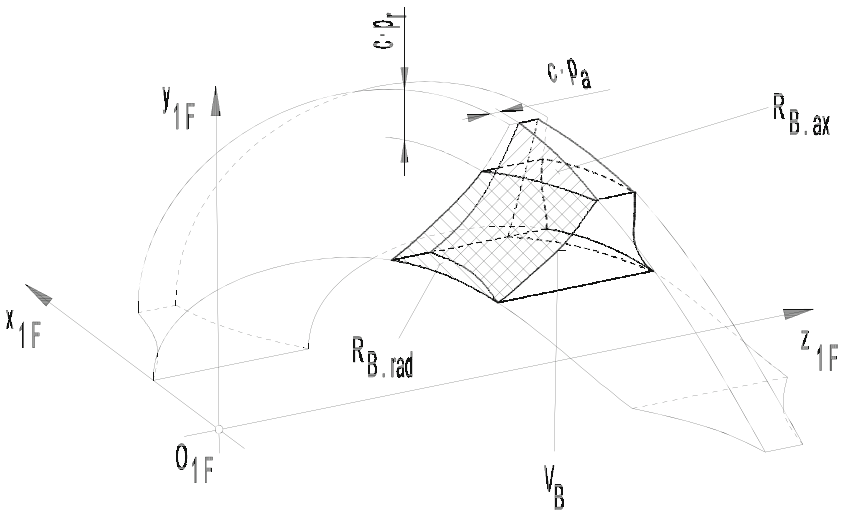

Fig. 9 The cutting edge of the tooth surfaces of the hob in the rotation coordinate system [9]

During our research work, we have elaborated a method to ensure the possibility of the examination of the wearing of the cutting edge of the hob in case of worms with arched profile.

The wearing of the cutting edge of the hob can be checked by CCD cameras in the production process in order to achieve precision manufacturing. The basis of precise examination with two CCD cameras in theory is Monge mapping. If photos of a spatial curve are taken with first and second CCD cameras placed in perpendicular direction in comparison to each other, then these fit to the projected images of the first and second image planes of the Monge mapping (Fig. 10).

The examination of the cutting edge curve can only be supported with CCD cameras if any piece of the curve can be unambiguously reconstructed from its two pictures (Fig. 11).

The condition of the reconstruction of the curve is that it does not have tangent line directed toward the projection line (Fig. 12) as described in Sect. 3. In case of this Monge projection of the curve, every projection line cut only one point from the first image curve and only one point from the second image curve; therefore, the spatial position of every point can be localized from two pictures.

If the curve has a tangent line parallel with profile direction, then there is a projection line in perpendicular position to axes x_{12} cutting two points from the first image of the curve and two points from the second image of the curve. In this case, the right connection of the images is not unambiguous; therefore, the localization of the spatial position of the curve is not possible only from its two pictures, as it was described in Sect. 3 (Fig. 13).

The right location of the CCD cameras is an indispensable and necessary condition for the examination of the wearing of the cutting edge of the hob, so that the reconstruction of any piece of the curve could be done unambiguously from only two of its pictures.

To ensure the reconstruction, the position of the CCD cameras must be calculated by using an interpolated curve to the

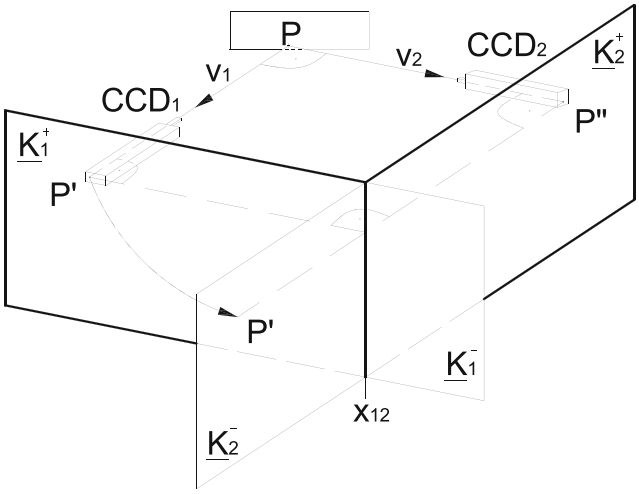

Fig. 10 The connection between the photos taken by CCD cameras and the Monge mapping

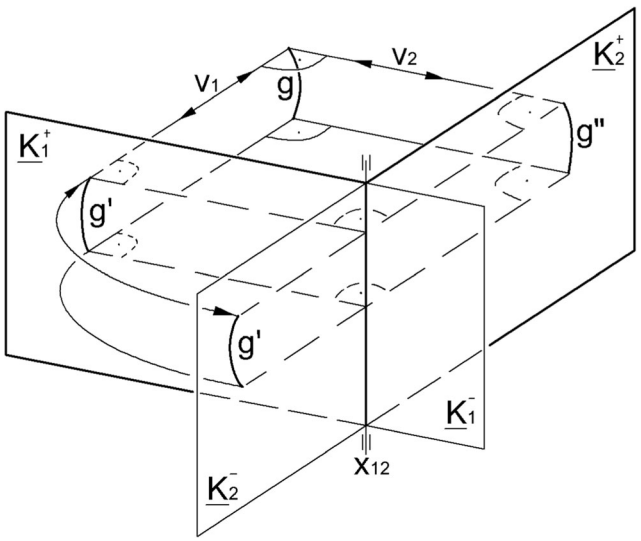

Fig. 11 The reconstruction of the curve from its two pictures

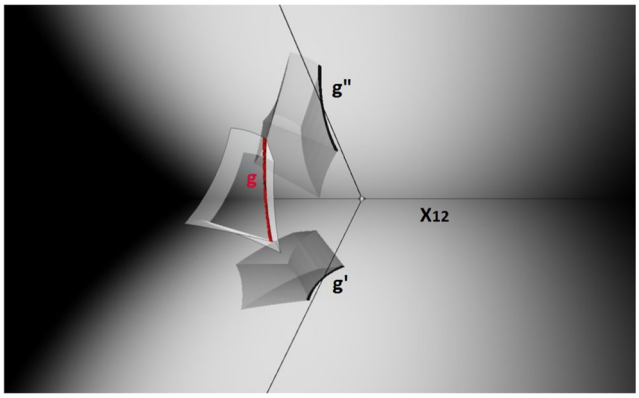

Fig. 12 A bijective Monge projection of the cutting edge of the hob

cutting edge. According to our previous examinations [12], the third-degree Bezier curve approaches the cutting edge within the permitted tolerance, if the four points of the cutting edge are selected proportionally between the addendum and dedendum cylinders to determine the interpolating Bezier curve. They must be supplied with proportional length of chord parameters. The third-degree Bezier curve fitted to the selected four points on the cutting edge in such a way results in a correct approaching of the cutting edge curve. The bijectivity of the third degree Bezier curve is examined in Sect. 4. The Monge projection of the third-degree Bezier curve interpolated to the cutting edge of the hob is interpreted by the photos taken by CCD cameras according to Figs. 9 and 10. The wearing examination can be done exactly by CCD cameras from the position that ensures reconstruction. If positions of CCD cameras to the Bezier curve interpolated to the cutting edge of the hob are determined by three free parameters from the non-bijective part of the Monge cuboid (Fig. 13), the curve has such a part, which cannot be reconstructed only from two pictures. If positions of CCD cameras to the Bezier curve interpolated to the cutting edge of the hob are determined by three free parameters from the bijective part of the Monge cuboid (Fig. 12), any part of the curve can be reconstructed only from two pictures.

With this method, the possibility for the continuous monitoring of the dimension change of the wearing of the cutting edge of the tool was given during the production process by us [3, 11].

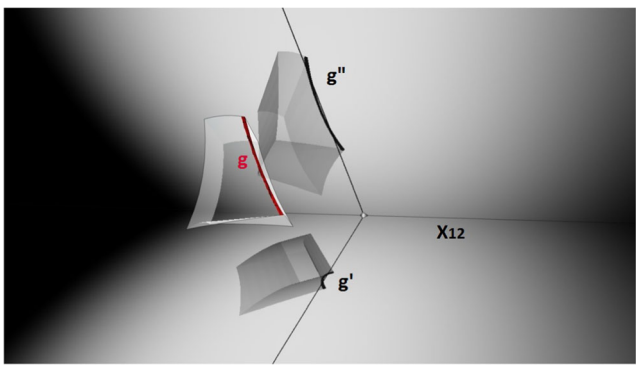

Fig. 13 A non-bijective Monge projection of the cutting edge of the hob

6 Summary

The research work gives a solution to the anomalies concerning the concept of the reconstruction problem of Monge projection with a procedure developed by us. Monge projections, which can be translated into each other, with parallel dislocation were considered identical; this way, the Monge projections can be described by three free real parameters. The three free real parameters are defined by the direction angles of projection lines of Monge projections in a fixed Descartes coordinate system. One triplet of free real parameters corresponds to one Monge projection and vice versa.

The applied triplets of free parameters have created the Monge cuboid. The Monge cuboid has two subsets. The bijective subset has points that give us those Monge projections in which the given cubic curve can be reconstructed. The non-bijective subset has other points that give us those Monge projections in which the given cubic curve cannot be reconstructed only from its two pictures. The bijective and non-bijective parts of the inside points of the Monge cuboid are bordered by points of second degree surfaces with respect to the given cubic curve. The method gives possibility for feedback during the machining of the cutting edge of the hob and continuous monitoring of the wearing of the cutting edge in order to determine the re-sharpening by using CCD cameras.

References

1. Chen F, Brown GM, Song M (2000) Overview of three-dimensional shape measurement using optical methods. Int J Adv Manuf Technol Opt Eng 39(1):10–22. doi:10.1117/1.602438 ISSN: 1433-3015 (electronic version)
2. Hilfert T, König M (2016) Low-cost virtual reality environment for engineering and construction. Res Vis Eng 4(2):18 . doi:10.1186/s40327-015-0031-5ISSN: 1433-3015 (electronic version)
3. Jadidi H, Ravanshadnia M, hosseinalipour M, rahmani F (2015) A step-by-step construction site photography procedure to enhance the efficiency of as-built data visualization: a case study. Vis Eng 3(3):12 . doi:10.1186/s40327-014-0016-9ISSN: 1433-3015 (electronic version)
4. Petrich, G (1973) *Descriptive geometry*, Budapest.
5. Balajti ZS (1995) *Examination of the bijectivity of the Monge projection* (in Hungarian) dr. univ. dissertation, First draft, Miskolc.
6. Drahos I (1988) The two-view drawing in the epoch of computational geometry. Proceedings ICEGDG Vienna l:117–121
7. Balajti, ZS (2015) *Theoretical examination of Monge projection and application in engineering practice,* Miskolc., ISBN: 978–963–358-097-4, p. 101
8. Balajti, ZS (2015) *The bijectivity of Monge projections in the production process of the arched worm gear,* 3rd International

Scientific Conference on Advances in Mechanical Engineering (ISCAME), in Debrecen, Hungary, ISBN: 978–963–473-917-3, pp.: 151–159

9. Dudás I (2004) *The theory & practice of worm gear drives,* Kogan Page US, Sterling, USA, ISBN 1 9039 96619 9, p. 320
10. Varga GY, Balajti ZS, Dudás I (2005) Advantages of CCD camera measurements for profile and wear of cutting tools. J Phys Conf Ser 13:159–162. doi:10.1088/1472-6596/13/1/037 Institute of Physics Publishing London
11. Dudás I, Bodzás S, Balajti ZS (2015) Geometric analysis and computer aided design of cylindrical worm gear drive having arched profile. Int J Innov Res Eng Manag (IJIREM) 2(5):10–14 ISSN: 2350-0557
12. Balajti, ZS (2007) *Development of production geometry of kinematics drive pairs* (in Hungarian), PhD dissertation, First draft, Miskolc. p: 181
13. Balajti, ZS, Bányai, K (2004) *A possibility method for the solve of 3D evaluation with 2 CCD cameras.* Miskolc, Production Process and Systems, A Publication of the University of Miskolc, Miskolc University Press. pp.: 237–242., 2002. HU ISSN 1215–0851
14. Dudás I (2016) The extension of the general mathematical model developed for helicoidal surfaces to the whole system of manufacturing technology and production geometry (ProMAT), The International Journal of Advanced Manufacturing Technology. Int J Adv Manuf Technol 82(1–4):16 . doi:10.1007/s00170-015-8233-5Springer, ISSN 0268-3768
15. T026566 sz. OTKA 2002 *Development of CCD cameras systems to the area of machine industry.* Miskolc. (Theme manager: Prof. Dr. Dr. h. c. DUDÁS Illés DSc.)